



University of Kentucky
UKnowledge

University of Kentucky Master's Theses

Graduate School

2004

OPTIMIZING GROWTH CONDITIONS FOR CHEMICAL VAPOR DEPOSITION OF SINGLE-WALLED CARBON NANOTUBES

Stanton W. McVay

University of Kentucky, smcve2@uky.edu

[Right click to open a feedback form in a new tab to let us know how this document benefits you.](#)

Recommended Citation

McVay, Stanton W., "OPTIMIZING GROWTH CONDITIONS FOR CHEMICAL VAPOR DEPOSITION OF SINGLE-WALLED CARBON NANOTUBES" (2004). *University of Kentucky Master's Theses*. 250.
https://uknowledge.uky.edu/gradschool_theses/250

This Thesis is brought to you for free and open access by the Graduate School at UKnowledge. It has been accepted for inclusion in University of Kentucky Master's Theses by an authorized administrator of UKnowledge. For more information, please contact UKnowledge@lsv.uky.edu.

Abstract of Thesis

OPTIMIZING GROWTH CONDITIONS FOR CHEMICAL VAPOR DEPOSITION OF SINGLE-WALLED CARBON NANOTUBES

Carbon nanotubes present enormous potential for future nanoelectronic applications. This study details one method for producing such nanotubes via chemical vapor deposition (CVD) of methane gas at high temperatures. This method represents the best known way to selectively place nanotubes, as will be needed for complex electronic structures. Various growth conditions are manipulated and the effects on the resulting nanotubes are recorded.

KEYWORDS: Nanotube, CVD, Chemical Vapor Deposition, Methane, Growth

Stanton W McVay

Author's Signature

December 2, 2004

Date

OPTIMIZING GROWTH CONDITIONS FOR CHEMICAL
VAPOR DEPOSITION OF SINGLE-WALLED CARBON
NANOTUBES

By

Stanton W. McVay

Dr Zhi Chen

Director of Thesis

Dr YuMing Zhang

Director of Graduate Studies

December 2, 2004

Date

RULES FOR THE USE OF THESES

Unpublished theses submitted for the Master's degree and deposited in the University of Kentucky Library are as a rule open for inspection, but are to be used only with due regard to the rights of the authors. Bibliographical references may be noted, but quotations or summaries of parts may be published only with the permission of the author, and with the usual scholarly acknowledgments.

Extensive copying or publication of the thesis in whole or in part also requires the consent of the Dean of the Graduate School of the University of Kentucky.

A library that borrows this thesis for use by its patrons is expected to secure the signature of each user.

Name

Date

THESIS

Stanton Wright McVay

The Graduate School
University of Kentucky
2004

Optimizing Growth Conditions for Chemical Vapor Deposition of Single-Walled Carbon Nanotubes

THESIS

A thesis submitted in partial fulfillment of the requirements for the degree of Master of Science in the College of Engineering at the University of Kentucky

By

Stanton Wright McVay

Lexington, KY

Director: Dr Zhi Chen, Professor of Electrical Engineering

Lexington, KY

2004

Copyright © Stanton W McVay

Acknowledgements

I would like to thank:

- Dr Zhi Chen for his support in this research, and for his invaluable advice and guidance

- Pang Leen Ong, Swee Yeaw Goh, Chi Lu, Dr Jun Guo, Dr Hongguo Zhang, Dr Dongyan Ding, and Alex Meece for their contributions and friendship

- George Spiggle, for providing support in the use and maintenance of Center equipment, and for helping with the assembly of our furnace system

- Larry Rice and Dr Alan Dozier for their training and assistance in the use of SEM and TEM microscopy

- Wentao Xu for his expertise in the use of electron-beam lithography

Table of Contents

ACKNOWLEDGEMENTS	III
TABLE OF CONTENTS	IV
TABLE OF FIGURES	VI
1.0 INTRODUCTION	1
1.1 Physical Properties of Nanotubes	3
1.2 Electrical Properties of Nanotubes	5
1.2.1 Rapid Thermal Annealing of Titanium	6
1.2.2 Palladium Contacts	7
1.3 Electronic Applications of Nanotubes	8
1.4 Barriers to Widespread Adoption	9
2.0 METHODS OF PRODUCTION	11
2.1 Arc-Discharge Synthesis	11
2.2 Laser Ablation Synthesis	12
2.3 Techniques for Selective Placement	14
2.3.1 AC Electric Field Alignment	14
2.3.2 Surface Functionalization with Polar Groups	14
2.4 Chemical Vapor Deposition	16
3.0 EXPERIMENTAL RESULTS	17
3.1 Experimental Overview	17
3.2 Apparatus	18
3.3 Catalyst and Substrate Preparation	20
3.4 Chemical Vapor Deposition	21
3.4.1 Pre-Bake Purge	21
3.4.2 Ramp Up	21
3.4.3 Chemical Vapor Deposition	21
3.4.4 Post-Bake Purge	21
3.4.5 Cleaning the Furnace Tube	22
3.5 Sample Imaging	23
3.5.1 SEM Sample Preparation	23

3.5.2 TEM Sample Preparation	23
3.6 Discussion of Results	24
3.7 Summary of Early Work	29
3.8 Modified CVD – Amorphous Carbon Prevention	30
3.9 TEM Imaging of SWNTs	32
3.10 Observed Characteristics of CVD-Grown NTs	35
3.10.1 Length vs Time and Temperature	35
3.10.2 Length vs Time and Flow Rate	37
3.10.3 Nanotube Starts per Catalyst Length, Constant Temperature	38
3.10.4 Nanotube Starts per Catalyst Length, Constant Flow Rate	39
3.10.5 Direction of Growth – Direct Observation	40
3.10.6 Catalyst Thickness	43
4.0 CONCLUSIONS	44
4.1 Summary of Findings	44
4.2 Suggestions for Future Research	46
5.0 REFERENCES	47
6.0 VITA – STANTON WRIGHT MCVAY	49

Table of Figures

FIGURE 1 - TEM IMAGE OF SINGLE-WALL CARBON NANOTUBES (SWNTS) ENTANGLED WITH CATALYST PARTICLES.	1
FIGURE 2 - VARIOUS CONFIGURATIONS OF SWNTS. (A) ARMCHAIR, N=M (B) ZIGZAG, M=0 AND (C) CHIRAL [REF 2]	3
FIGURE 3 - SCHEMATIC ILLUSTRATION OF THE GENERATION OF A NANOTUBE BY FOLDING OF A SECTION OF A GRAPHITE SHEET [REF 5]	4
FIGURE 4 (A) A SUGGESTED LAYOUT FOR A SINGLE-MOLECULE SWNT NAND GATE. RED REGIONS ARE POLYSILICON GATES, BLUE REGIONS ARE METAL INTERCONNECTS. (B) THE CORRESPONDING SCHEMATIC REPRESENTATION	6
FIGURE 5 - DIAGRAM OF AN INVERTER FABRICATED FROM A SINGLE SWNT [REF 7]	8
FIGURE 6 - A CNT-BASED MEMORY CELL, BASED ON SONOS TECHNOLOGY [REF 12]	9
FIGURE 7 - SCHEMATIC REPRESENTATION OF THE ELECTRIC-ARC APPARATUS USED AT THE UNIVERSITY OF MONTPELLIER (FRANCE) [REF 13]	11
FIGURE 8 - DIAGRAM OF THE LASER ABLATION PROCESS FOR NANOTUBE GROWTH [REF 18]	12
FIGURE 9 - THE CVD REACTOR BUILT FOR THIS PROJECT	18
FIGURE 10 - CVD GROWN NTS WITH A RANGE OF DIAMETERS. NOTE THE SMALLER DIAMETERS CLOSER TO THE SURFACE.	25
FIGURE 11 - CLOSEUP OF TWO NANOTUBES. THE LOWER TUBE TAPERS AND EXTENDS TO TOP OF THE IMAGE. THE UPPER TUBE TAPERS AND DISAPPEARS TO THE LEFT, PROBABLY BEFORE REACHING THE IMAGE EDGE.	26
FIGURE 12 - THE TUBE SEEN HERE EXHIBITS A TYPICALLY FLAKY APPEARANCE.	26
FIGURE 13 - THE TUBE IN THE CENTER OF THE PICTURE APPEARS TO HAVE BEEN SEVERED. IT SEEMS LIKELY THAT A REMNANT IS PRESENT, THOUGH NOT VISIBLE, WHICH IS SUPPORTING THE TUBE.	27
FIGURE 14 - TEM IMAGE SHOWING A CROSS-SECTION OF A CARBON TUBE STRUCTURE. THE BLACK OVALS ARE GOLD COLLOID PARTICLES OF ROUGHLY 20NM DIAMETER.	28
FIGURE 15 - A CARBON TUBE WITH SEVERAL VARIATIONS IN ITS DIAMETER	30
FIGURE 16 - TEM IMAGE SHOWING TWO SWNTS. ONE IS AT CENTER-RIGHT, THE OTHER ALONG THE LEFT EDGE OF THE IMAGE. BOTH HAVE A DIAMTER OF 2-3NM. THESE WERE GROWN AT 900 C.	32
FIGURE 17 - TEM IMAGE SHOWING A SWNT PROTRUDING FROM A CATALYST MASS. THE TUBE IS TO THE LEFT OF THE BLACK LINE. GROWTH TEMPERATURE WAS 900 C	33
FIGURE 18 - SEVERAL SWNTS ARE SHOWN HERE, GROUPED INTO ROPES OR BUNDLES. THESE WERE GROWN AT A TEMPERATURE OF 850 C	34
FIGURE 19 – HISTOGRAM OF TUBE LENGTHS FOR A SAMPLE GROWN AT 900 C FOR 20 MINUTES	36
FIGURE 20 – GRAPH OF TUBE LENGTH VS TIME AND GROWTH TEMPERAURE	36
FIGURE 21 – GRAPH OF TUBE LENGTH VS TIME AND FEEDSTOCK CONCENTRATION	37
FIGURE 22 – GRAPH OF NANOTUBE POPULATION VS TIME AND FEEDSTOCK CONCENTRATION	38
FIGURE 23 - GRAPH OF NANOTUBE POPULATION VS TIME AND TEMPERATURE	39
FIGURE 24 - CATALYST PATCH WITH NANOTUBES GROWING IN ALL DIRECTIONS	40
FIGURE 25 - WHILE THE SURFACE AREA OF A CNT DEVICE MAY BE RATHER SMALL, ITS EFFECTIVE SURFACE AREA IS MUCH LARGER, DUE TO THE UNCONTROLLED GROWTH OF UNNEEDED TUBES	41
FIGURE 26 - A SUGGESTED MEANS OF CONTAINING EXTRA CNTS	42
FIGURE 27 - THE UPPER IMAGE SHOWS A MUCH THICKER CATALYST PATCH, AND A RESULTING INCREASE IN THE NUMBER OF TUBES. THE LOWER IMAGE SHOWS A THINNER CATALYST LAYER WITH FEWER TUBES.	43

1.0 Introduction

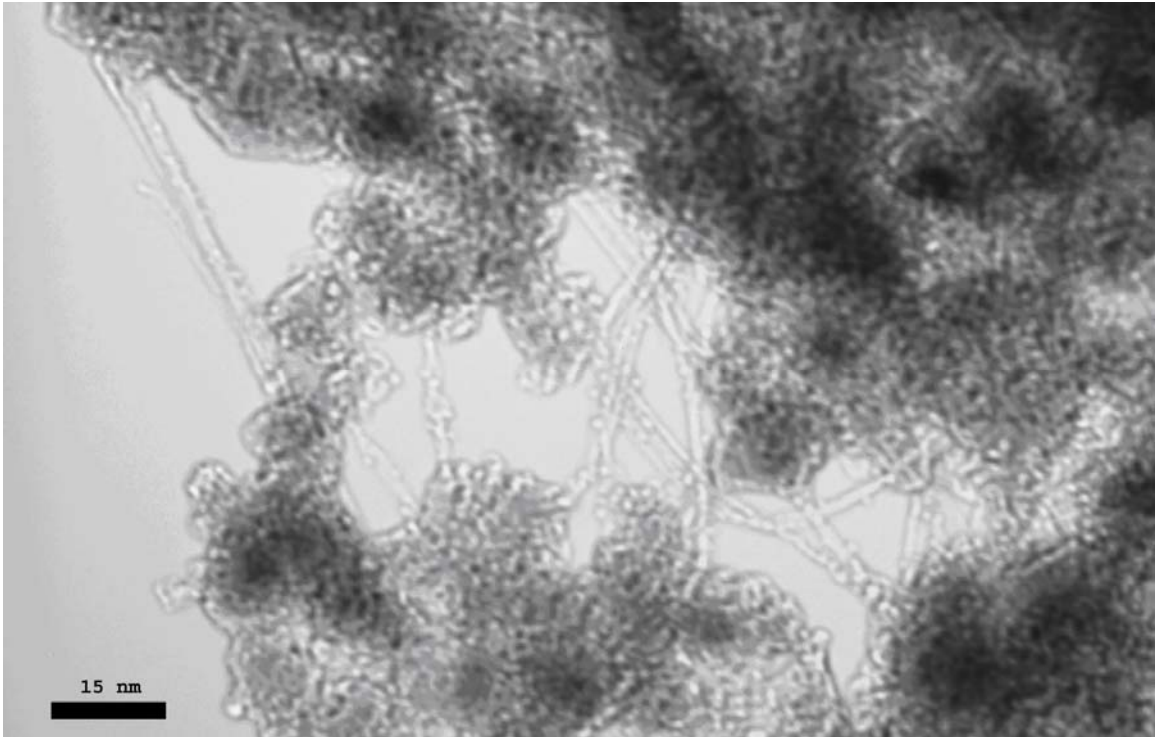


Figure 1 - TEM image of single-wall carbon nanotubes (SWNTs) entangled with catalyst particles.

First discovered by Sumio Iijima in 1991 [1], carbon nanotubes (CNTs) have been the subject of intense research in recent years. Such nanotubes are molecules of carbon atoms arranged in a cylindrical fashion, often with diameters of 1 nm or less. These nanotubes have remarkable mechanical and electrical properties. Not least is their ability to function as nanoscale transistors and conductors [2].

Before being used as nanoscale devices, nanotubes must first be precisely located and contacted with electrodes. Having such small size is an advantage for miniaturizing electronics, but has proven a great difficulty in application. Hence, it is desirable to find ways to produce carbon nanotubes directly on a given position on a substrate.

One such method is chemical vapor deposition, or CVD [3]. While bulk tubes can be produced using a powdered or gaseous catalyst, CVD can also grow tubes directly onto a

substrate, in positions determined by patterned catalyst particles. This technique has great potential for opening up microelectronics to carbon nanotube devices [4].

For this project, a CVD reactor will be constructed and CVD growth of carbon nanotubes will be performed. These tubes will then be examined, to determine how the various growth parameters affect the final output.

This report will briefly discuss the known science of nanotubes, the problems involved in utilizing nanotubes in electronics applications, and the various means of producing nanotubes. Also, one such means of production, chemical vapor deposition (CVD) is explored and experimental results are discussed.

1.1 Physical Properties of Nanotubes

A carbon nanotube is a long, thin structure of concentric tubes of carbon atoms with a diameter on the nanometer scale. Since they can reach lengths on the micron scale, and therefore aspect ratios in the thousands, CNTs are often treated as one-dimensional structures. CNTs closely resemble another form of carbon, graphite, with a similar six-sided crystalline structure. Where graphite has a planar structure, CNTs appear as graphite wrapped into a cylinder [2].

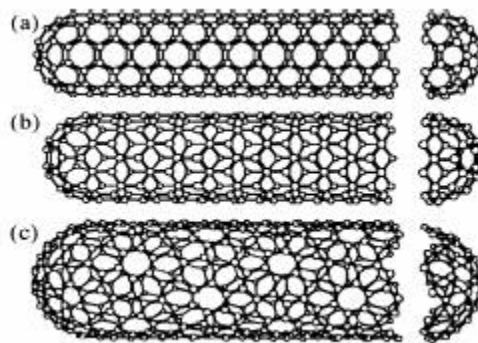


Figure 2 - Various configurations of SWNTs. (a) Armchair, $n=m$ (b) Zigzag, $m=0$ and (c) Chiral [Ref 2]

The simplest carbon nanotube is a single-walled nanotube (SWNT). Consisting of a single carbon shell, these small structures have been recorded with diameters smaller than 1 nm. As seen in Figure 2, these SWNTs come in a variety of orientations. This orientation is expressed in a quantity called chirality.

Chirality is denoted by a 2-digit identifier, (n,m) . In this identifier, n and m are multipliers for the unit vectors of graphite [5]. See Figure 3. In the example shown, a nanotube of chirality $(5, 2)$ is shown as a portion cut from a graphite sheet. In the figure, $5 \cdot a_1 + 2 \cdot a_2$ lattice units separate the two points A and B. If these two points were to be pulled together, the resulting nanotube would have chirality $(5, 2)$. The vector C is the circumference of the resulting tube, and the vector P is parallel to the length of the tube [5].

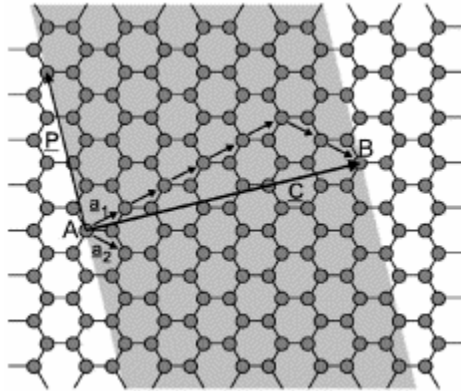


Figure 3 - Schematic illustration of the generation of a nanotube by folding of a section of a graphite sheet [Ref 5]

More complex nanotubes are also possible. Multi-walled carbon nanotubes (MWNTs) are structures of concentric SWNTs. Each tube has its own chirality, so a combination of various types is possible [2].

1.2 Electrical Properties of Nanotubes

Based on their chirality, a nanotube can be either metallic or semiconducting. If $n=m$, or if $n-m=3i$, where i =any integer, then the tube is effectively metallic. This means that it can conduct current regardless of whether a bias voltage is present. Otherwise, the tube is semiconducting, with a band gap of $E_{\text{gap}} = 4/3 h v_f / d_{\text{cnt}}$ where d_{cnt} is the tube's diameter, h is Planck's constant, and v_f is the Fermi velocity.

For the case of multi-wall nanotubes, each shell of the overall structure has its own chirality. Thus, most multi-wall nanotubes are effectively metallic, as the probability of having all semiconducting component shells is low. One metallic shell effectively renders the whole structure metallic [5].

By themselves, SWCNTs are inherently p-type semiconductors. However, annealing in vacuum or inert gases can render them n-type [5], or even ambipolar [6]. Ambipolar CNTs will conduct for a strong bias voltage of either polarity.

The polarity does not need to be constant for a single tube. By passivating part of a tube, and annealing the whole, the passivated region can be made n-type while the balance remains p-type. The resulting structure behaves as an inverter, all in a single molecule [7].

More complicated logic gates may also be possible. An extremely long semiconducting nanotube could be selectively doped or passivated and annealed to produce regions of a specific polarity. In theory, gates such as NANDs or NORs could be realized in this fashion. A suggested layout for a NAND is shown in Figure 4.

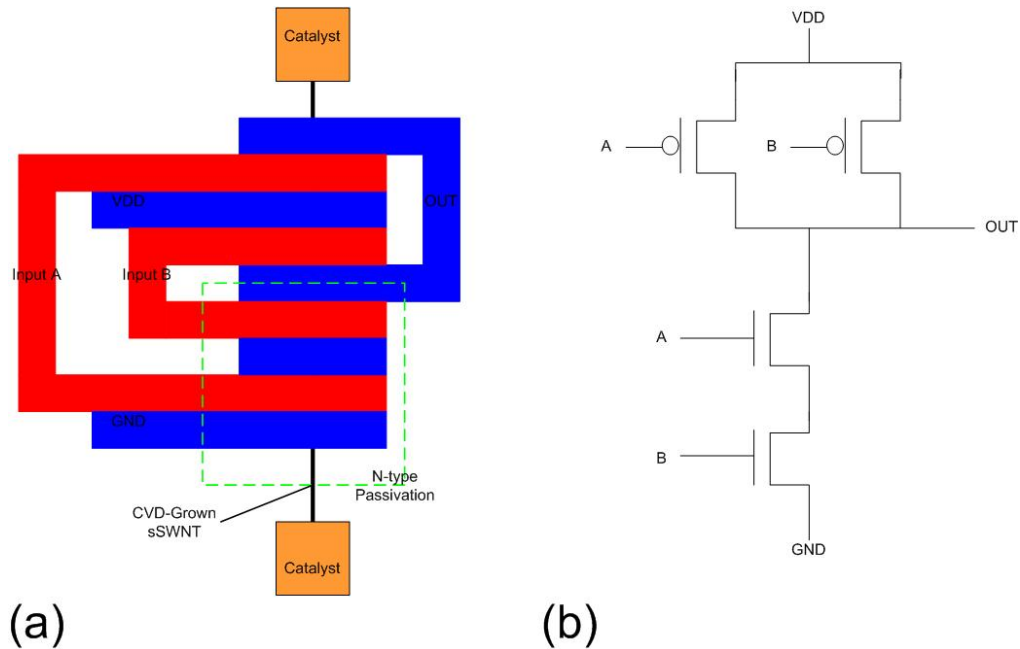


Figure 4 (a) A suggested layout for a single-molecule SWNT NAND gate. Red regions are polysilicon gates, blue regions are metal interconnects. (b) The corresponding schematic representation

SWNTs by themselves are excellent conductors. Metallic SWNTs have a resistance of just 6.5kOhm, or two units of quantum conductance, $4e^2/h$ [8]. Here, e denotes the electron charge and h denotes Planck's constant. This opens the possibility of ballistic (non-scattering) transistors made from semiconducting SWNTs. However, to be useful, metal contacts must be used to connect to the ends of the tube. These contact resistances have proven to be rather high, as well as unpredictable [9]. Some contacting techniques have proven to have very low contact resistances.

1.2.1 Rapid Thermal Annealing of Titanium

One study has demonstrated that focusing an electron beam on a metal contact would reduce its contact resistance by a few orders of magnitude [10]. Using an electron beam in this fashion is impractical for large patterns of contacts. Lee, et al achieved ohmic contacts of titanium and cobalt using a rapid thermal annealing (RTA) technique [9]. Most titanium contacts on CNTs, for example, stabilized naturally at 10MΩ. When the

samples were placed in a vacuum chamber and annealed at 600-800C for just 30s, the contact resistance dropped to 0.5 to 50 k Ω , and remained stable for several months.

1.2.2 Palladium Contacts

Such an annealing technique does, however, require an extra step to produce such low contact resistances. Another group has determined that palladium contacts naturally form ohmic contacts with nanotubes [8], with no annealing step required. Such devices exhibit overall resistance (two contacts and the tube itself) of 32k Ω . This provides good contact resistances, but it is noted that palladium itself is not especially durable. For applications where the contacts will be directly probed, it is best to apply an additional metal layer, such as titanium.

1.3 Electronic Applications of Nanotubes

Work has been done to take advantage of the similarity between semiconducting SWNTs and conventional MOS transistors. Such nanotube transistors are called CNTFETs, or carbon nanotube field-effect transistors. Simple logic systems have been constructed with these CNTFETs as the active elements.

Though by nature p-type, n-type SWNTs can be made by vacuum annealing. A group in the Netherlands fabricated NMOS logic in such a fashion, with off-chip pull-up resistors. In this way, they were able to build NMOS inverters, NORs, simple memory cells, and ring oscillators [11].

Such devices are hampered by the fact that they utilize off-chip resistances. A better way would involve on-chip resistances, or even better, CMOS logic. Such gates have also been fabricated. Taking advantage of the variable doping of a SWNT, CMOS logic can be realized using a single tube. Different parts of the tube can have different polarities, so the same tube can be treated as both p-type and n-type. An inverter created in such a way is shown below [7].

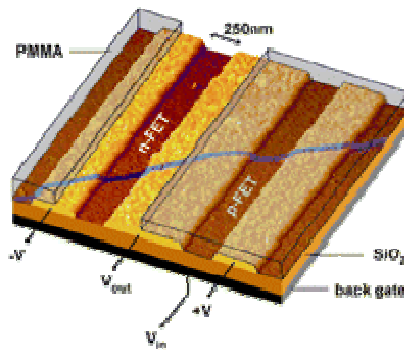


Figure 5 - Diagram of an inverter fabricated from a single SWNT [Ref 7]

Nanotube-based memory devices have also been fabricated. A team of researchers in Korea fashioned a non-volatile memory cell with a semiconducting SWNT as a channel. Similar in structure to a MOSFET, this memory cell uses a 3-layer film in place of the

gate oxide. This film is composed of a Si_3N_4 layer sandwiched between two SiO_2 layers. A cross-section and top view is shown below [12].

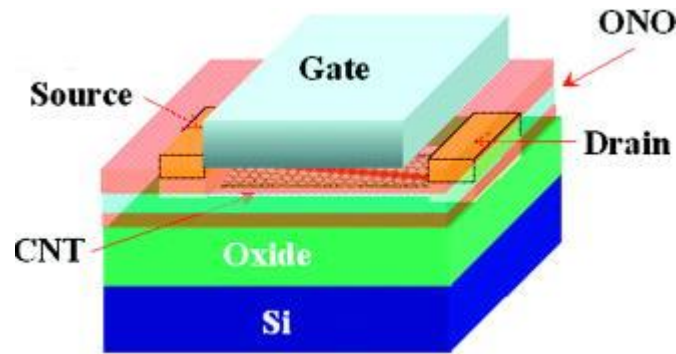


Figure 6 - A CNT-based memory cell, based on SONOS technology [Ref 12]

1.4 Barriers to Widespread Adoption

Devices such as those described above are formed in one of two ways. First, by forming electrical contacts and directly placing a nanotube there using an atomic force microscope (AFM). Second, by scattering nanotubes at random on a substrate and using an in-situ patterning method such as electron beam lithography to pattern electrodes directly on an individual tube.

While these are useful for proof of concept experiments, they are impractical for large scale production of nanotube devices. Before nanotube electronics can be made commercially viable, a number of problems must be solved:

1. Placement – Nanotubes by the thousands or millions must each be placed in the correct location on a substrate.
2. Numbers – In a given location, the selective placement technique must provide finite, repeatable numbers of nanotubes (perhaps exactly one nanotube).

3. Specificity – The correct type of nanotube (semiconducting or metallic) must be placed in each location. Further, semiconducting tubes must be of a predictable band-gap.

This report will consider the various nanotube production methods available in light of these problems.

2.0 Methods of Production

2.1 Arc-Discharge Synthesis

Arc Discharge experiments were the first known source of carbon nanotubes, and led to their original discovery in 1991. This technique involves creating an arc of electrical current between two carbon electrodes. The intense heat of the arc vaporizes carbon at the anode, and causes it to crystallize as CNTs at the cathode. One such apparatus is shown below. [13]

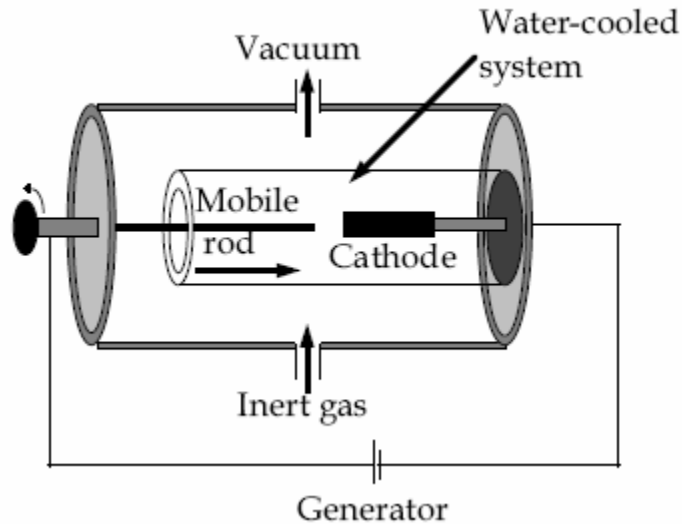


Figure 7 - Schematic representation of the electric-arc apparatus used at the University of Montpellier (France) [Ref 13]

Several experimental conditions can be changed to control the qualities of the tubes produced. The proportions of inert gas ambient have been shown to affect the diameter of the resulting tubes, as the atmosphere influences how quickly the carbon atoms recool after vaporization [14]. The applied voltage and resultant current, and their consistency, have also been shown to influence the nanotubes [15].

In addition, research has shown that single-wall nanotubes can result if the carbon anode is doped with metal atoms, such as Fe, Ni, or Co. During vaporization, the carbon atoms

are absorbed into the metal particles and from there begin to re-crystallize as SWNTs [16].

Arc discharge remains a useful method for bulk production of carbon nanotubes. However, the exact nature of the resulting tubes is not constant. Additionally, while efforts at improving selectivity are paying off, this method offers no direct means for manipulation of tubes.

In terms of the problems of nanotube electronics, this method provides no answer to the problem of placement, or the problem of numbers. Improving control of nanotube production, however, does hold potential for solving the problem of specificity.

2.2 Laser Ablation Synthesis

Laser ablation is similar to arc discharge, in that a carbon source is vaporized so that carbon atoms can reform as nanotubes. In this method, the energy source is a laser beam and the carbon source is a graphite target. The laser strikes the target, vaporizing the carbon which re-crystallizes and forms nanotubes [17]. A typical laser ablation apparatus is shown below.

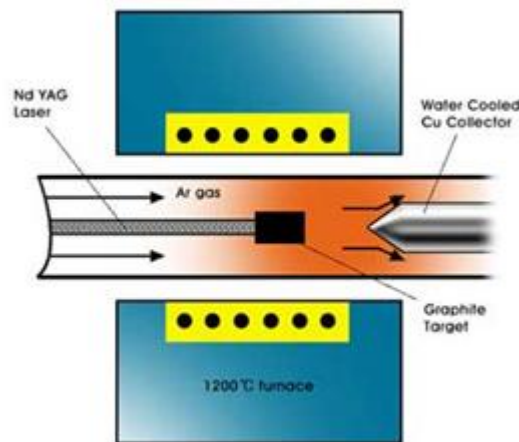


Figure 8 - Diagram of the laser ablation process for nanotube growth [Ref 18]

As with arc discharge, SWNTs can result if the carbon target is doped with metals such as Co, Fe, Ni, or Y. The resulting soot is composed of SWNTs, plus some MWNTs, carbon fibers, and/or amorphous carbon [19].

Like the arc-discharge method, this method provides no answer to the problem of placement, or the problem of numbers. There has been promising work done, however, in producing specific types of nanotubes, with potential for solving the problem of specificity.

2.3 Techniques for Selective Placement

Arc-discharge and laser ablation synthesis are similar in that they provide bulk nanotubes. To be useful in large-scale electronic applications, a way must be found to selectively place nanotubes on a substrate. Some groups have suggested ways to place nanotubes formed by bulk production methods. In conjunction with methods like arc-discharge and laser ablation, these techniques suggest solutions to the problem of placement.

2.3.1 AC Electric Field Alignment

Krupke, et al has shown that metallic nanotubes can be aligned between metal electrodes using AC electric fields [20]. This phenomenon occurs because of the difference in dielectric constants of semiconducting and metallic tubes. Semiconducting tubes have a dielectric constant less than 5. Metallic tubes, on the other hand, have extremely large dielectric constants.

By suspending a mixture of the two tube types in a solvent of a dielectric constant between the two extremes and applying an AC electric field, the semiconducting tubes are repelled while metallic tubes are attracted. This could allow metallic tubes to be placed in a desired location, to create a low-resistance bridge between two points.

This technique does not, however, work well for large-scale separation of metallic and semiconducting tubes. The actual number of metallic tubes removed from solution is small, so this method is lacking as a means to purify semiconducting tubes.

2.3.2 Surface Functionalization with Polar Groups

Collaboration between American and Korean research groups has produced a novel method of selective placement of nanotubes [21]. In this method, chains of organic molecules are used to pattern the surface. Polar chemical groups, such as amino or

carboxyl, placed on a substrate tend to attract nanotubes in solution. Conversely, non-polar groups, such as methyl, have been shown to repel nanotubes.

It has also been shown that once a single nanotube has attached itself to a polar region, it has a repelling effect on other tubes. Thus, it appears that this method also has potential to ensure exactly one nanotube in a given location. At publication, over 70% of such regions in experiments had just one nanotube in each polar location.

2.4 Chemical Vapor Deposition

In essence, Chemical Vapor Deposition (CVD) of carbon nanotubes is the decomposition of hydrocarbon gases such as methane or ethylene [24]. A catalyst in powder form [23] or spread on a substrate [22] is placed inside a furnace. The furnace is heated and the hydrocarbon gases (called feedstock) are introduced. When the feedstock enters the heated furnace, it decomposes in the presence of catalyst into hydrogen gas and free carbon atoms. The hydrogen flows out of the furnace along with most of the carbon atoms, but some carbon atoms coalesce on the furnace walls or on the catalyst.

Carbon that reaches the catalyst is absorbed into the metal particles. When these particles become saturated with carbon, the carbon begins to crystallize. As more carbon becomes available, this crystal lengthens into a carbon nanotube. It has been shown that the resulting nanotube has a diameter roughly equal to that of its parent particle.

While earlier work focused on bulk production of nanotubes on powder catalyst, work has also been done with patterned catalyst on a substrate. The properties of the catalyst are the same in this arrangement, but far less is present and thus far fewer tubes are grown. One group has used such CVD to grow nanotubes directly on top of existing electrodes [22].

By growing the nanotubes directly onto a substrate, CVD provides a possible solution to the problem of placement. It is uncertain, but one could surmise that careful formulation of the catalyst material could help control the problem of numbers, as well. While CVD does not provide a direct means of controlling the properties of nanotubes. The diameter of catalyst particles can be controlled, however, raising the possibility of controlling the diameter and thereby the chirality of CNTs [25]. This would be a potential solution to the problem of specificity. Since CVD suggests solutions to all three problems stated earlier, it is the focus of this project.

3.0 Experimental Results

3.1 Experimental Overview

The purpose of this research is to determine the feasibility of CVD growth of carbon nanotubes for electronics purposes. To form a nanotube transistor, for example, one SWNT is sufficient and even ideal. A larger number might also be acceptable, if each tube had the same properties and if the number was consistent across the process.

This project relies heavily on the work of two published sources. A group at Stanford University reported the synergistic properties of iron and molybdenum as SWNT catalyst material [24]. Another group first showed that low temperatures and feedstock flow rates would produce SWNTs as surely as more wasteful processes [23].

To begin, the experimental procedures of these groups were re-created to produce SWNTs. Once this was done in bulk, the same process was applied to patterns of catalyst. The relative frequency and length of tubes were noted to help characterize the growth process.

3.2 Apparatus

Experimental Setup:

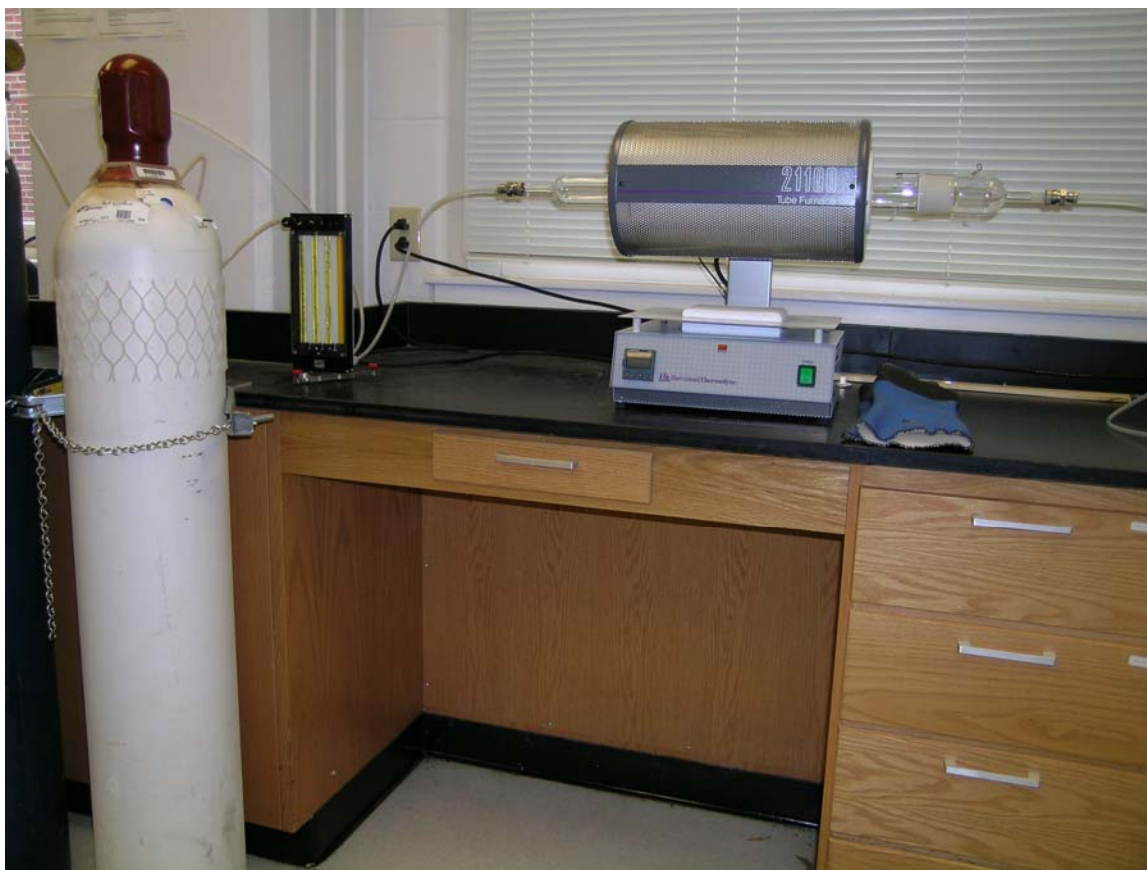


Figure 9 - The CVD reactor built for this project

The equipment used in CVD synthesis of carbon nanotubes is shown here. The components are as follows:

1. Feedstock and purge gases – There are currently 2 hydrocarbon gases available: methane and acetylene. Hydrogen is also present, but was not found to have any effect on nanotube growth. Argon is used for purging and for diluting feedstock concentration. Gases are purchased from Scott-Gross Co in Lexington, KY.

2. Gas flow control and mixer – This device has flowmeters for up to 3 gases, and a valve to control the flow of each. After leaving the flowmeters, the gases are blended and then fed into the furnace tube.
3. Furnace tube – custom ordered from Quartz Scientific. This is a 2” diameter quartz tube. One end is removable for sample access. The ends are fitted with Swagelock fittings for the ¼” tubing.
4. Furnace – Thermolyne 21100. This is a single-zone furnace with a maximum temperature of 1200 C. Furnace temperature is controlled and monitored with a single set point controller.
5. Exhaust – After leaving the furnace, the gases are filtered through liquid paraffin and cooled in water before flowing into the nearby fume hood outtake.

3.3 Catalyst and Substrate Preparation

In this project, a Fe-Mo catalyst was used. Fe catalyst has been shown to stimulate CNT growth, but only after a lengthy reduction step with hydrogen gas to convert iron oxides to elemental iron particles. The presence of Mo, however, allows Fe to produce NTs without a reduction step [24]. It has also been shown that a Fe:Mo ratio of 5:1 works best [23].

It is not desirable to have only Fe-Mo present in the catalyst. To provide bulk and spacing between particles, alumina nanoparticles of 30nm diameter are used. The catalyst solution was prepared by mixing these chemicals:

Chemical	CAS	Quantity
Methanol	67-56-1	30 mL
Alumina nanoparticles	N/A (from Degussa)	30 mg
Ferric Nitrate, nonahydrate	7782-61-8	30 mg
$C_{10}H_{16}MoO_6$	17524-05-9	6 mg

The alumina nanoparticles were acquired from Degussa. Iron was provided in the form of ferric nitrate nonahydrate, purchased from the university's chemical stockroom. Molybdenum was provided in the form $C_{10}H_{16}MoO_6$, purchased from Sigma-Aldrich. To prepare the catalyst solution, component compound powders are added to 30mL of methanol. The mixture was stirred for 24 hours and sonicated for 1 hour. To re-use the same solution later, it was re-stirred for at least 30 minutes. The catalyst solution was then applied to silicon substrates using a pipet. For fast evaporation of the methanol, the substrate was placed on a hotplate and heated to 80C. In this way, entire 2-inch silicon wafers can be prepared with catalyst, and then broken into pieces for CVD.

3.4 Chemical Vapor Deposition

3.4.1 Pre-Bake Purge

Before beginning the CVD process, it is crucial to remove all atmospheric air from the furnace tube. The presence of oxygen will result in the formation of CO₂ instead of atomic carbon during the heating process. To prevent this, the tube is purged with 1000mL/min of argon gas for 60 minutes prior to heating the furnace.

3.4.2 Ramp Up

Once the tube is purged of oxygen gas, the furnace temperature is set to the desired growth temperature. The furnace can heat up at a rate of 50 C/min. For a typical growth temperature of 850 C, 17-18 minutes are required to heat the furnace. During this ramp, the purge gas flow is maintained at 1000mL/min. Typically, the furnace is allowed to sit at the target temperature for another 5 minutes. This is to allow the furnace's "hot zone" to stabilize at the target temperature.

3.4.3 Chemical Vapor Deposition

When the target temperature has been reached, the feedstock gas can be introduced and the purge gas reduced. Typical flow rates for CVD are 360mL/min of argon with 40mL/min of methane. Currently, there is no true flow control, so these values must be maintained and corrected by hand. The feedstock is allowed to flow for a set period of time. For this project, values of 10-40 minutes were used.

3.4.4 Post-Bake Purge

An important step in the formation of SWNTs is the post-bake purge. After the required time has elapsed, the carbon feedstock gas is shut off and the argon purge gas is increased to 1000mL/min. Obviously, the ending of the feedstock source does not mean that there is no carbon gas in the tube. If the temperature is reduced immediately after shutting off the feedstock gas, the furnace will pass through lower temperatures with a carbon source

still present in the tube. This leads to a buildup of amorphous carbon on the entire substrate, including the previously formed carbon nanotubes. The result is an increase in the apparent diameter of the tubes. This phenomenon will be explained in more detail in a later section.

While this buildup is certainly ruinous to electronic applications, it does have a useful application in microscopy. Carbon nanotubes are normally too small to be resolved with scanning electron microscopes. With the carbon buildup, tubes can reach a diameter of 10nm or greater. This allows tubes to be seen via SEM, and some quantities, such as length and tube frequency, to be measured.

For the purposes of growing single-wall tubes for TEM imaging or electronic purposes, however, this buildup should be prevented. To do so, the temperature of the furnace is maintained for one hour after the feedstock gas is shut off. This removes all the carbon source gas from the tube before moving to lower temperatures. It should be noted for future users that doing so will limit the usefulness of SEM, as such small features would not be well-resolved, if visible at all. TEM imaging, however, will be able to show the single-wall tubes.

3.4.5 Cleaning the Furnace Tube

After CVD growth, a thin residue of carbon can become visible inside the furnace tube. This carbon build up can be easily burned off by heating the furnace to >800 C while flowing oxygen gas through the tube. The oxygen reacts with the carbon soot, forming carbon dioxide. This removes the carbon film and also removes a potential source of contamination from future CVD reactions.

3.5 Sample Imaging

3.5.1 SEM Sample Preparation

Scanning Electron Microscopy (SEM) is a useful tool for imaging the surface topography of a sample. The University of Kentucky has two SEMs: the Hitachi S-900 and S-3200. The S-3200 is much easier to use for relatively low magnification applications, with a maximum effective magnification of ~30000x. The S-900, while not as user-friendly as the S-3200, is capable of higher magnifications, up to ~100000x.

For both machines, the sample to be viewed must be adhered to a sample mount. These mounts are metallic, and provide both stability and a ground path for electrons. The sample is adhered to a mount using a layer of colloidal graphite (Ted Pella P/N 16053). For heavier samples, a two-sided conductive carbon tab can be used as well. After the sample is adhered to the mount, it is useful to apply more colloidal graphite along the edges of the sample. This ensures that electron charge will not build up on the sample, which could result in a distorted or unreadable image.

After imaging, the sample can be removed from the mount by gentle prying. The mount should then be cleaned with acetone to remove the residual graphite. It is also helpful to gently scrub the mount with fine-grit sandpaper until bare metal shows. This helps prevent contamination of the SEM chamber with residual graphite or sample materials.

3.5.2 TEM Sample Preparation

While SEM is a useful technique for imaging large-scale characteristics of tubes, such as length and diameter, it provides no insight into the inner structure of a sample.

Transmission Electron Microscopy (TEM) provides a cross-sectional view of a sample, revealing the sample's inner structure. For this project, the JEOL 2000FX and the JEOL 2010 F were used to confirm the presence of SWNTs.

Since the TEM works by projecting an electron beam through a sample, it is necessary to remove the catalyst and tubes from the substrate. This was done by scraping the catalyst from the substrate using a stainless steel scalpel. Since the tubes are anchored in the catalyst, they come away as well. The resulting black powder is dissolved in isopropyl alcohol and sonicated for 1 hour, to break up the catalyst into smaller pieces.

After sonication, the CNT solution is applied to a lacey carbon grid using a pipet. After evaporation, a drop of gold colloid particles is applied and allowed to evaporate. These particles are necessary to provide a calibration standard for TEM images, as the device itself provides no scale.

3.6 Discussion of Results

The first attempt made at CVD growth of nanotubes followed a procedure described by in reference 24. This called for a methane flow rate in the thousands of ml/min for 1 hour. When this growth attempt was made, the entire furnace turned black with soot within a couple of minutes, so the attempt was halted. When the sample was removed and examined under SEM, large carbon fibers were apparent, with diameters over 100nm. As well, interesting soot structures were present.

It seemed likely that too much feedstock was being used, so another procedure was necessary. Another group published a procedure with far smaller flow rates, as low as 40 mL/min [23]. This resulted in a far cleaner reactor, and noticeably smaller tube diameters. However, the carbon tubes were still much larger than SWNTs should be, with diameters in the tens of nanometers.

A closer examination of these structures showed several notable features. One was the inconsistency of the tube diameters. As shown in the SEM image in Figure 10, a variety of diameters can be present in the same region of the substrate.

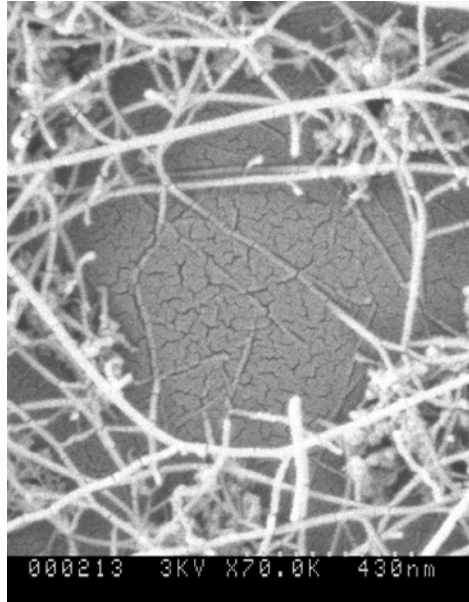


Figure 10 - CVD grown NTs with a range of diameters. Note the smaller diameters closer to the surface.

As seen in this example, the tube diameters vary from $\sim 40\text{nm}$ down to $\sim 10\text{nm}$. Another interesting point is that the tubes tend to be smaller closer to the substrate surface.

Inconsistencies have also been seen along the same tube. Some tubes demonstrate a clear tapering effect toward the ends or in their middle sections. The tube shown here has a maximum diameter of $\sim 30\text{nm}$, but thins at the tips to less than 10nm .

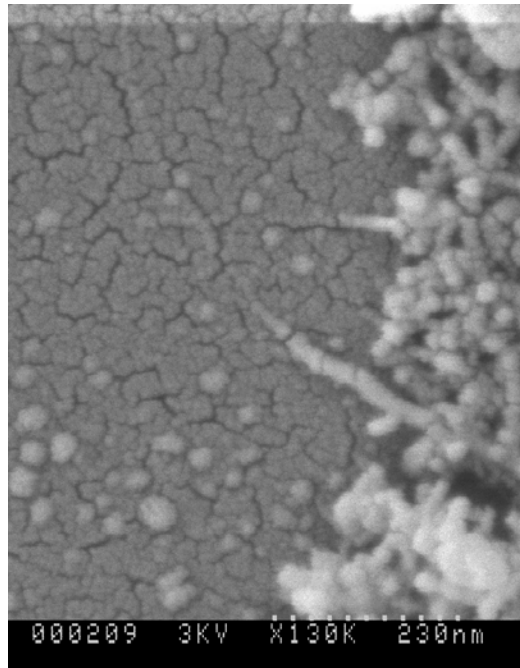


Figure 11 - Closeup of two nanotubes. The lower tube tapers and extends to top of the image. The upper tube tapers and disappears to the left, probably before reaching the image edge.

Another feature of these structures is the flaky quality of their walls. Under high magnification, most tubes exhibit frequent cracks or breaks. These breaks are always nearly perpendicular to the tube's length.



Figure 12 - The tube seen here exhibits a typically flaky appearance.

In some cases, the cracks appear to have severed the tube, but the tube maintains its position. This would seem to suggest a remnant is present that is not apparent to SEM.

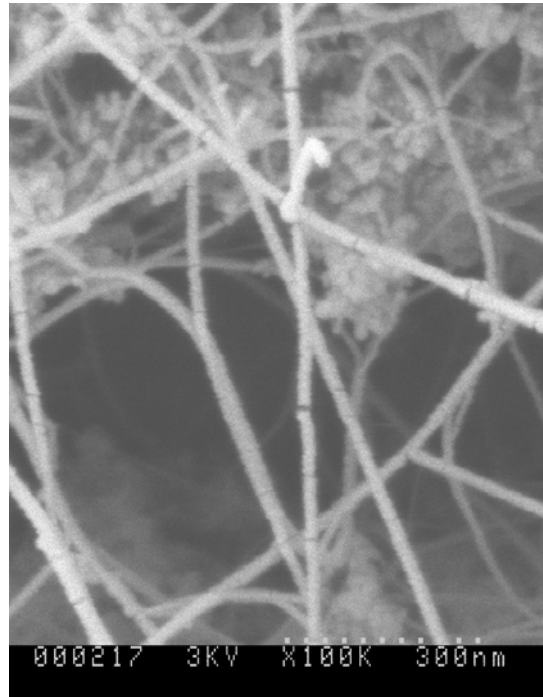


Figure 13 - The tube in the center of the picture appears to have been severed. It seems likely that a remnant is present, though not visible, which is supporting the tube.

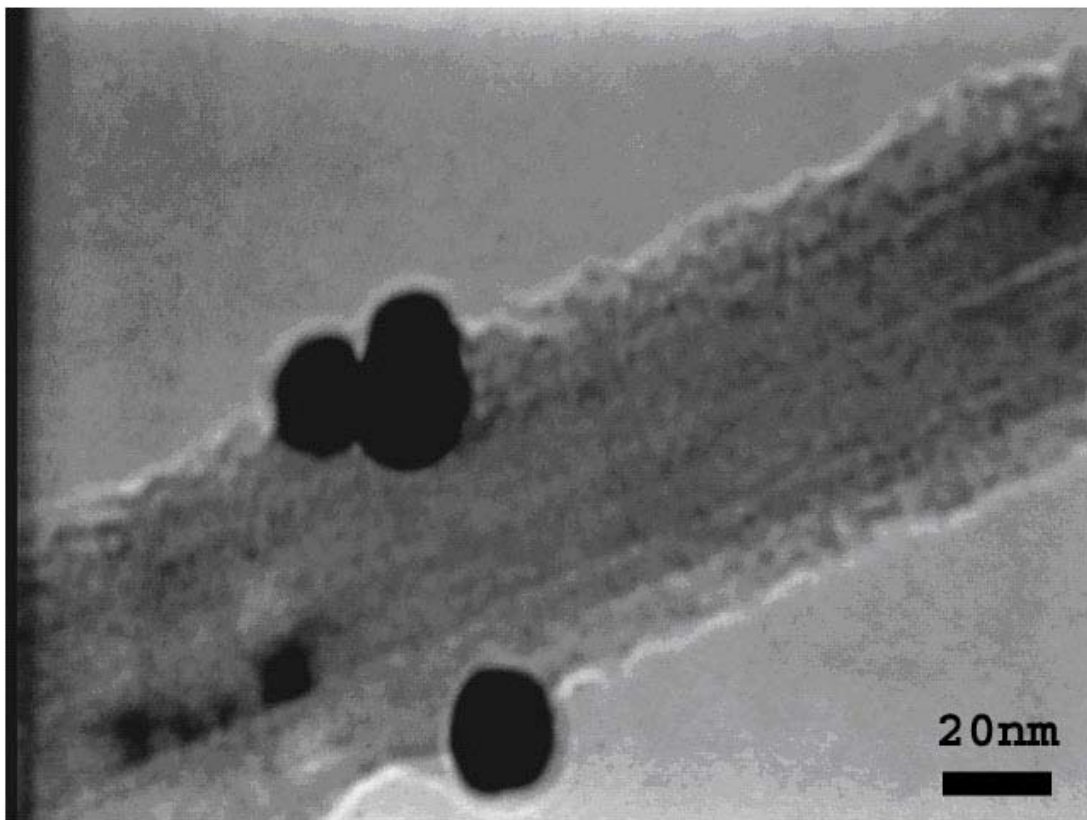


Figure 14 - TEM image showing a cross-section of a carbon tube structure. The black ovals are gold colloid particles of roughly 20nm diameter.

Under TEM, it appears that another structure is contained within these larger fibers. The outer layers appear amorphous, which may also explain the flaky nature of this outer region in SEM images. The tube shown here has a diameter of roughly 60nm. The outer edges clearly show an amorphous nature, as no crystalline structure is apparent. The inner layer or layers do show some definition, evident in the thin lines running the length of this feature. The lines that are visible appear to be straight and parallel, suggesting a MWNT or perhaps a parallel bundle of SWNTs.

3.7 Summary of Early Work

To summarize the findings thus far:

1. CVD of methane does produce tubelike structures on Fe-Mo catalyst at 800-900C, at relatively low flow rates.
2. These tubes are much larger than SWNTs are expected to be.
3. The tubes themselves are highly variable, with changing diameters and frequent gaps and breaks along their lengths.
4. The internal structure of these tubes is amorphous on the outside, with some structure inside.

These findings seem to indicate that nanotubes may be present, but are coated in a thick layer of amorphous carbon. This would seem to explain the inconsistent nature of the tubes under SEM, and the amorphous/crystalline structure seen under TEM.

But where does this coating come from? The publications on which this work was based make no mention of this phenomenon, much less its prevention. Clearly something was taken for granted, or left unmentioned. A closer look at the experimental procedure is necessary.

3.8 Modified CVD – Amorphous Carbon Prevention

Another observation was made, based on SEM imaging.

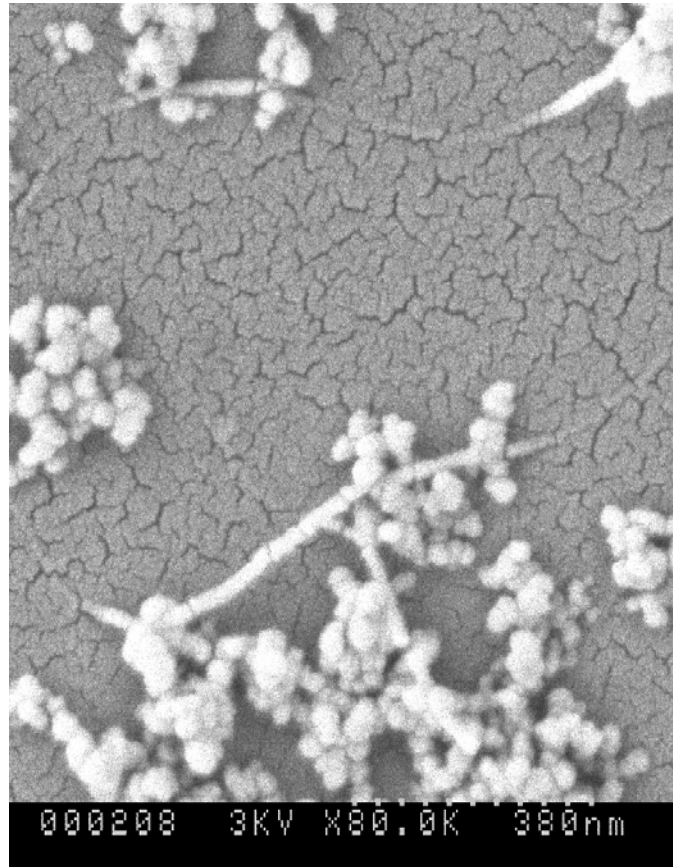


Figure 15 - A carbon tube with several variations in its diameter

This image shows a single tube which has a highly variable diameter. At its widest, it appears to be at least 30nm in diameter. It then tapers in several places to less than 10 nm, and becomes hard to see at this magnification.

If this structure was grown all at once, it seems unlikely that it would exhibit such an inconsistent diameter. A thick tube at the base tapering to a narrow tip might be possible, but such wild variation along its length seems very unlikely. More likely, the underlying crystalline structure (SWNT or MWNT) grows first and reaches full length. At some

point afterward, the amorphous carbon grows or is deposited on the underlying nanotubes.

The tapering effect of the tubes as they get closer to the surface may be explained by a nanoscale equivalent of ground effects. That is, the flow of gases is nearly constant far above the surface of the substrate. Closer to the surface, where the catalyst introduces variation in elevation, the flow rate might not be a constant. It is also possible that most of the available carbon was already absorbed upstream of the thinner tubes.

From previously published works, we know that the nanotubes themselves grow at high temperature under feedstock gas, in this case methane. So, it stands to reason that the coating comes at some point after this high temperature growth.

The growth procedure up to this point had involved flowing methane gas into the reactor at high temperature, followed by cooling the tube while purging with argon. Due to its small size, the furnace used can heat up and cool down rather quickly. It seemed reasonable, then, that the reactor could be cooling down faster than the methane could be purged. At lower temperatures, the decomposition of methane would not necessarily form new nanotubes.

As it happens, another, older source explained the growth of thick (~1 μ m) carbon fibers in this way [26]. So the problem then becomes to maintain a high temperature until the methane is cleared out of the tube, so that no amorphous carbon gets a chance to form. This is done easily by purging the reactor with argon for several minutes before allowing the system to cool down.

As will be shown in the next section, doing this has an interesting side effect. While SWNTs are now apparent under TEM, without their carbon sheathing they are too small to resolve in SEM.

3.9 TEM Imaging of SWNTs

Without the thick sheath of amorphous carbon, the underlying structure becomes apparent. As shown here, SWNTs are indeed grown from the Fe-Mo catalyst.

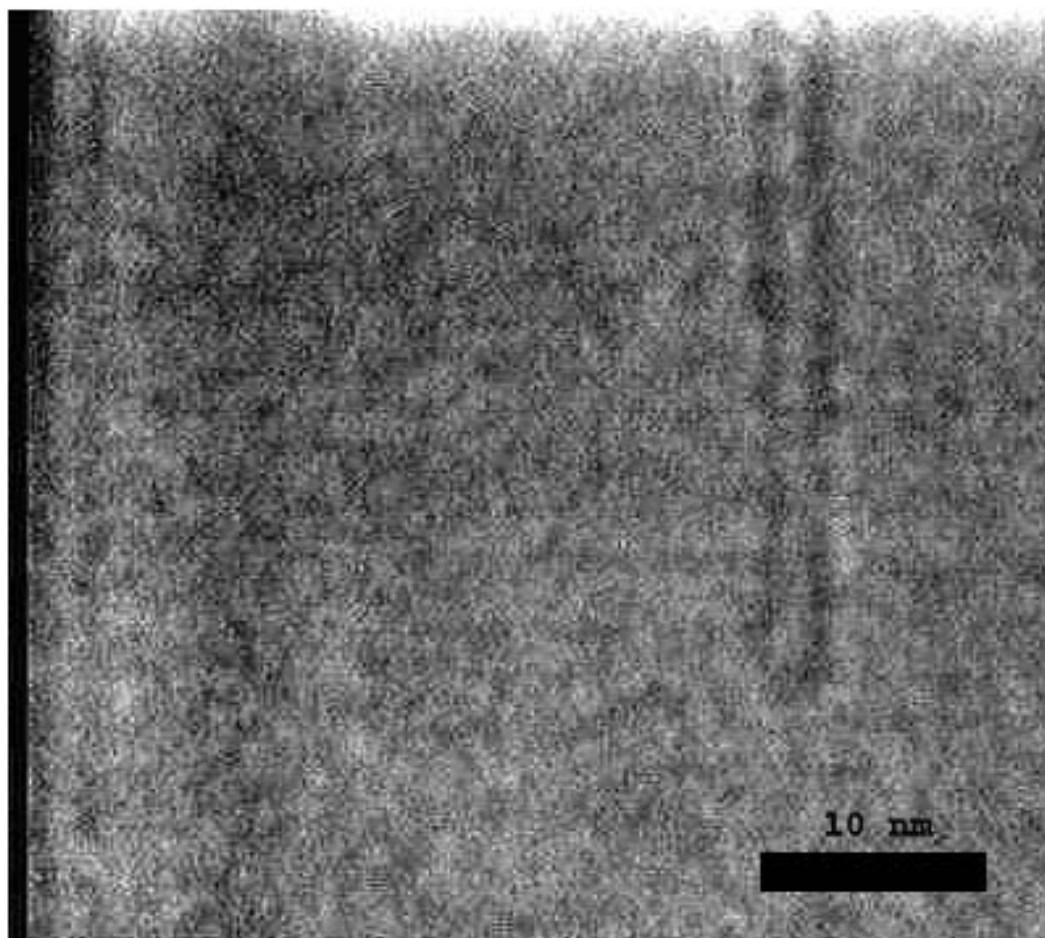


Figure 16 - TEM image showing two SWNTs. One is at center-right, the other along the left edge of the image. Both have a diameter of 2-3nm. These were grown at 900 C.

The TEM image shown here was taken at a magnification of ~3 million x. Two SWNTs are present (one is at the extreme left). The rounded end of one is also seen. It is noteworthy that the tubes seen in this way are not bundles, but rather individual tubes.

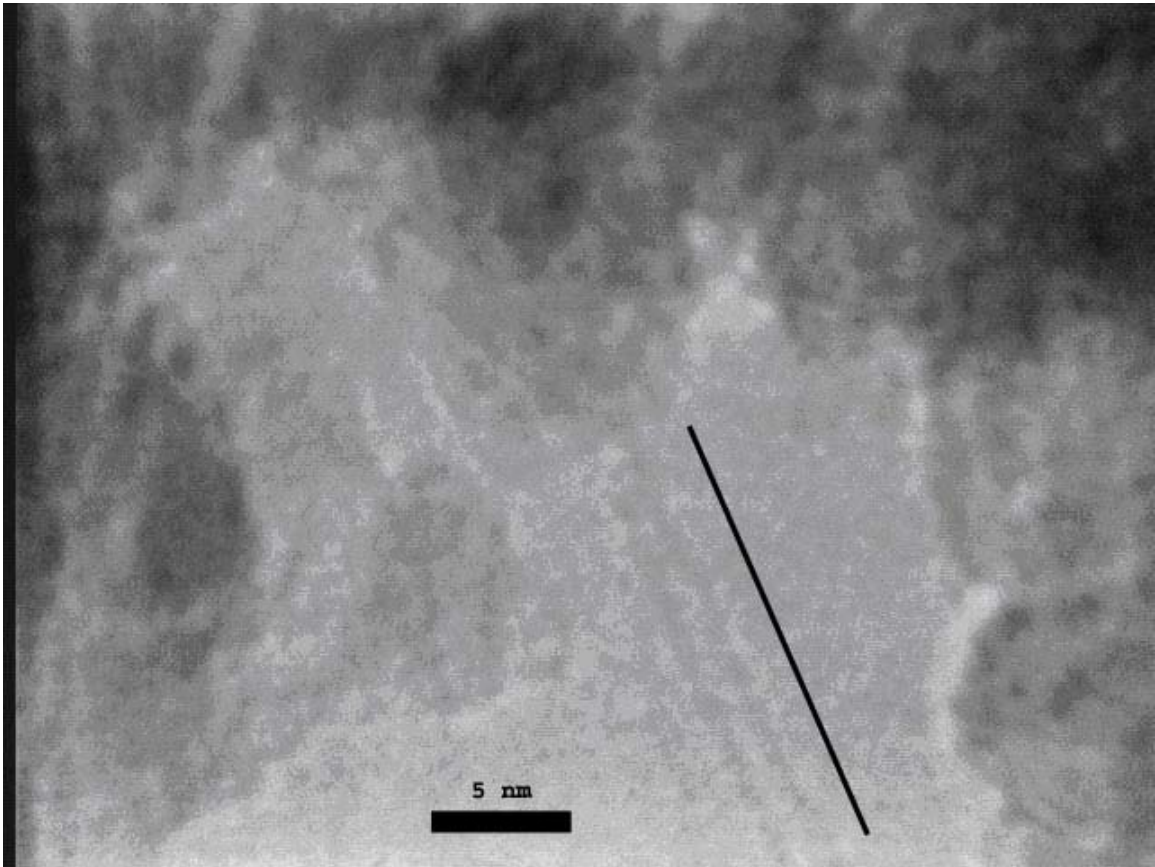


Figure 17 - TEM image showing a SWNT protruding from a catalyst mass. The tube is to the left of the black line. Growth temperature was 900 C

Here a tube is shown emerging from its catalyst. The presence of the catalyst complicated the imaging of the SWNTs. To prepare these samples, several drops of the catalyst were placed on the substrate and dried. This extra material tended to stick together, creating opaque regions on the TEM grid. This complicated the search for SWNTs. As shown here, the best place to look is along the edges.

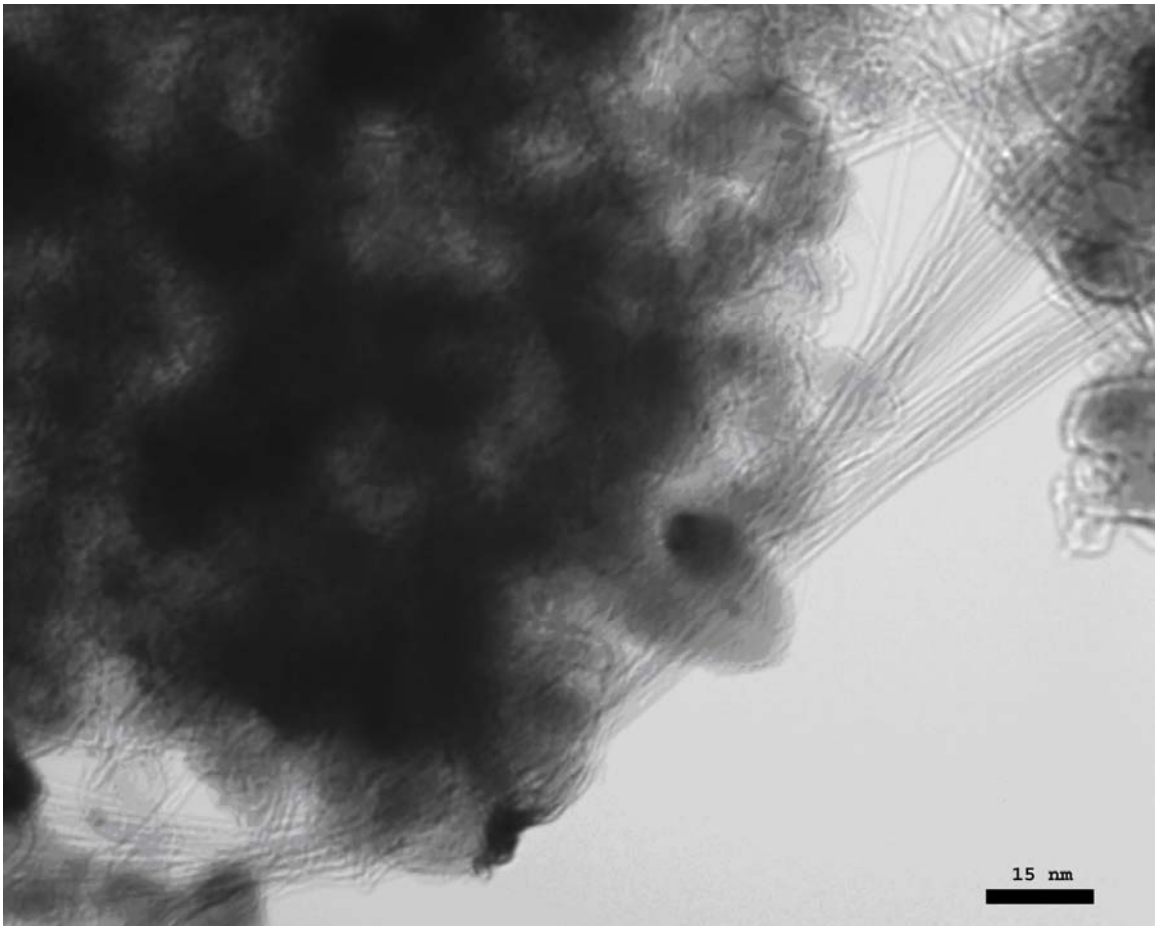


Figure 18 - Several SWNTs are shown here, grouped into ropes or bundles. These were grown at a temperature of 850 C

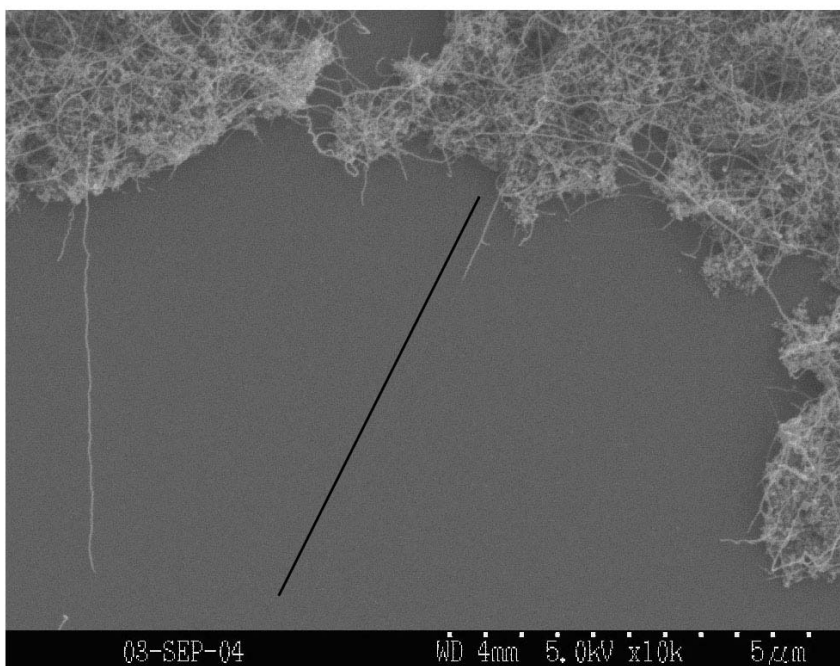
Here bundles of SWNTs can be observed. This image was made using a HRTEM. The tubes were grown at 850 C.

It is noteworthy that there are clear differences in the images of tubes grown at 900 C and 850 C. Granted, these images were taken using different instruments. However, the images of tubes grown at 900 C demonstrate individual tubes. The images of tubes (including Figure 1) grown at 850 C appear to be in bundles. While the instrumentation used may be responsible, it is also possible that the different growth regimes had an effect on the tubes produced, making bundles more or less likely.

3.10 Observed Characteristics of CVD-Grown NTs

3.10.1 Length vs Time and Temperature

The first parameter experimented with was the length of grown nanotubes as a function of reaction time. This time was varied from 10 to 40 minutes at temperatures of 800, 850 and 900 C. The resulting tubes were measured for length in several spots on each sample, with 40-50 tubes measured for each sample. The only tubes measured were those on the edge of a catalyst patch. Tubes in the interior are tangled, and may have been terminated prematurely. Feedstock concentration was kept at 10% methane/90% argon, with a combined flow rate of 400mL/min.



This sample was grown at 900C for 20 min. Care was taken to measure the entire length of each tube. For example, the long tube in the center beside the black guideline is 6.5um, but is coated for only about 1.5um of its length. A quick glance would underreport its length.

The measurements were then averaged for each combination of growth conditions. The length histogram for the preceding sample is shown here, followed by a chart of the mean length for each growth condition.

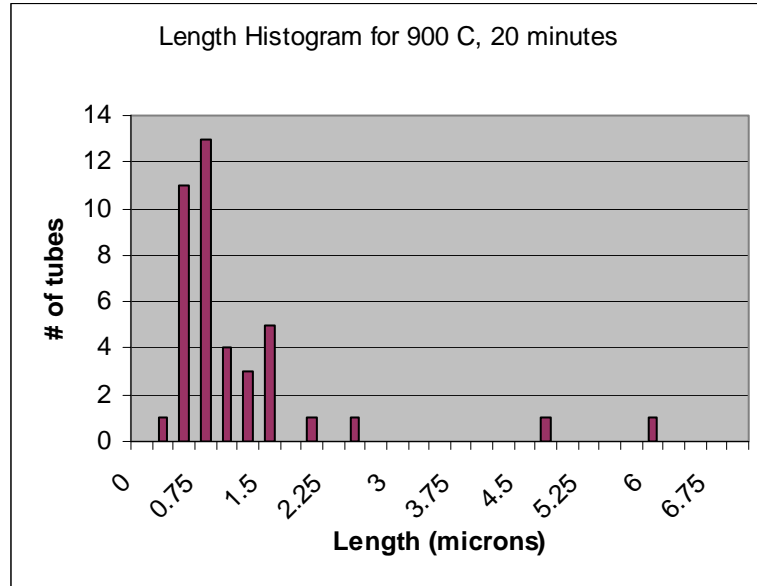


Figure 19 – Histogram of tube lengths for a sample grown at 900 C for 20 minutes

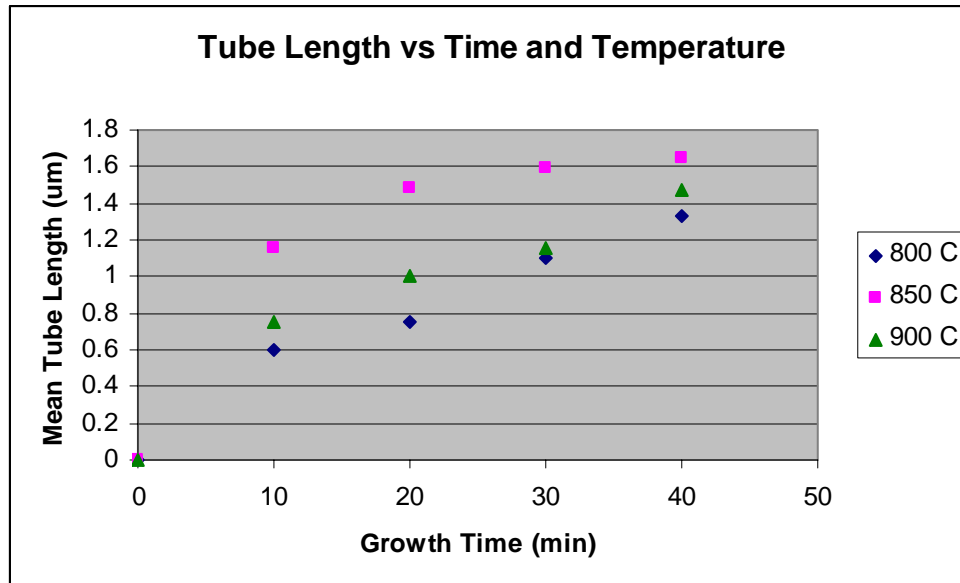


Figure 20 – Graph of Tube Length vs Time and Growth Temperature

As expected, longer growth times tended to produce longer nanotubes. However, the growth rate seems to decay exponentially as the tubes become longer. Most of the growth appears to take place in the first 20 minutes. Also interesting is that the peak growth temperature is not the highest; rather, the mean tube length is greatest at all times for a reaction temperature of 850 C.

3.10.2 Length vs Time and Flow Rate

In this trial, the flow rate of methane and argon was adjusted to produce different methane concentrations. Various times were also used, with results shown below. The growth temperature was kept at 900 C.

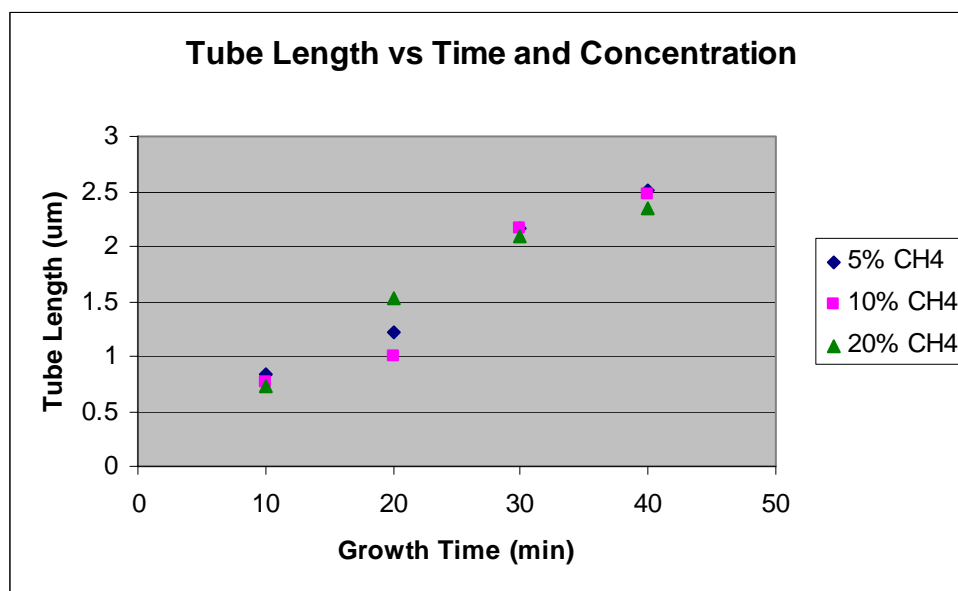


Figure 21 – Graph of Tube Length vs Time and Feedstock Concentration

In each case, a total flow rate of ~400 sccm was used, with argon for the balance of the feedstock. The mean tube length does not appear to be strongly dependent on the size of the methane component. This would seem to suggest that the 5% flow regime is close to a “saturation” level for this process, and that additional methane is not helpful in producing longer tubes.

3.10.3 Nanotube Starts per Catalyst Length, Constant Temperature

To determine a minimum catalyst region width to produce a fixed number of nanotubes, a metric must be found for how many tubes are expected per unit length of catalyst. In this trial, the number of tubes per length of catalyst was measured, disregarding the actual length of the tubes. In all cases, the growth temperature was held at 900 C.

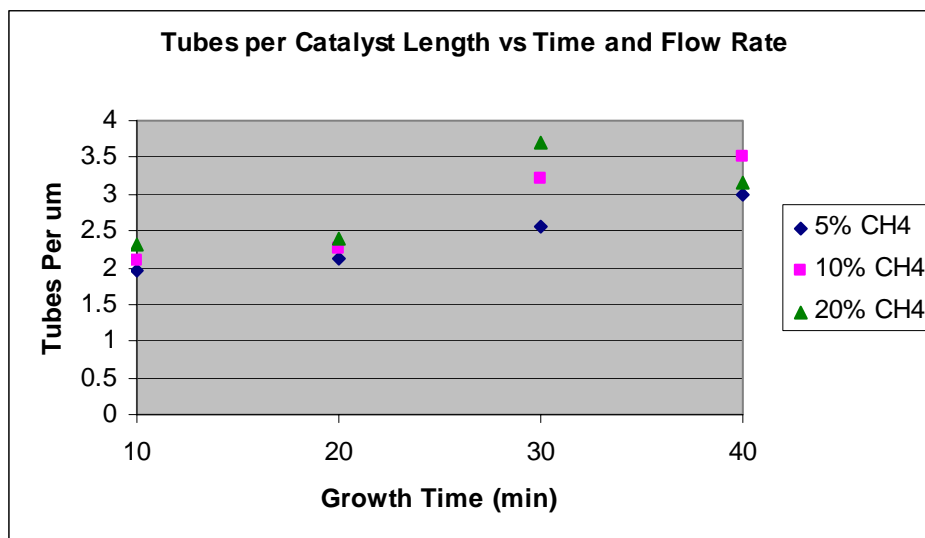


Figure 22 – Graph of Nanotube Population vs Time and Feedstock Concentration

The general trend is for the number of tubes to increase as the flow rate increases, and also to increase as the growth time lengthens. The rate of increase, however, is not great. It seems that most of the tubes originated in the first 10 minutes of growth, with only slight increase over the next 30 minutes. Also, while it does seem that a higher flow rate contributes to the number of tubes, the difference is not great. As found in the length trials earlier, it appears that increasing the flow rate beyond 5% methane does not produce a great improvement in the number of tubes grown.

3.10.4 Nanotube Starts per Catalyst Length, Constant Flow Rate

Another trial was performed to see the effect of varying temperatures on the number of tubes grown. In all cases, the flow rate was kept at 10% methane (40 mL/min CH₄ : 350 mL/min Ar).

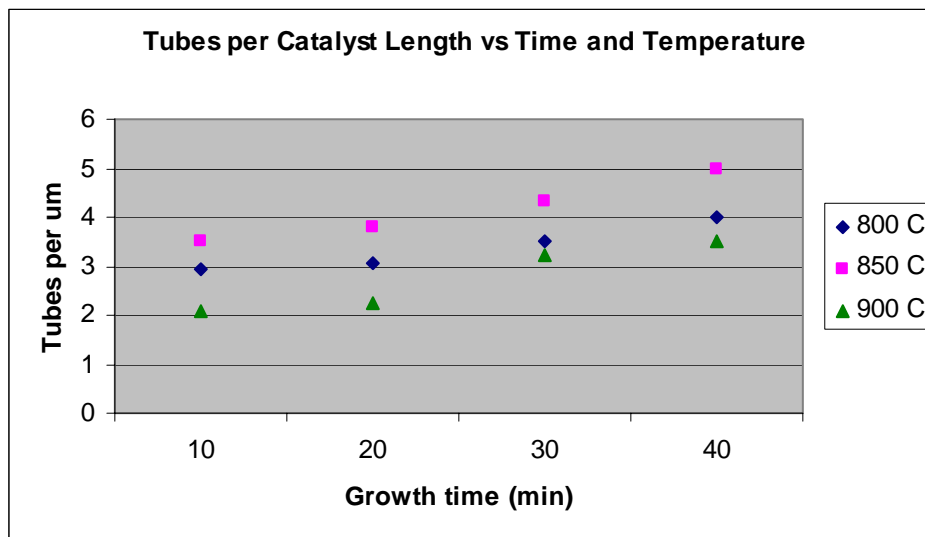


Figure 23 - Graph of Nanotube Population vs Time and Temperature

As with the previous trials, 850 C appears to be at or near optimum for tube growth. Again it is seen that while a longer reaction time produces some effect in the number of tubes, the difference is not great. Also, an interesting effect is seen in the other temperatures tested. In the length trials, it was found that 900 C produced consistently longer tubes than 800 C. However, here it appears that more tubes are actually grown at 800 C than 900 C.

It should be noted that this and the previous surveys were performed using SEM. Thus, the structures counted were those visible under SEM, which could be carbon-coated SWNTs or large bundles of tubes. So, this number is useful to illustrate the general trend that more tubes appear with longer reaction times and concentrations, but not necessarily accurate for a proper census of SWNTs per length.

3.10.5 Direction of Growth – Direct Observation

One reason that CVD is so attractive for CNT growth is that it offers the potential to create a nanotube exactly where it is needed. As shown here, CVD also introduces a potential problem, in that nanotubes will tend to grow from all directions from the catalyst. While not necessarily a problem for a single CNT device, it would seem to prevent any other devices from being formed in a certain radius around the catalyst.

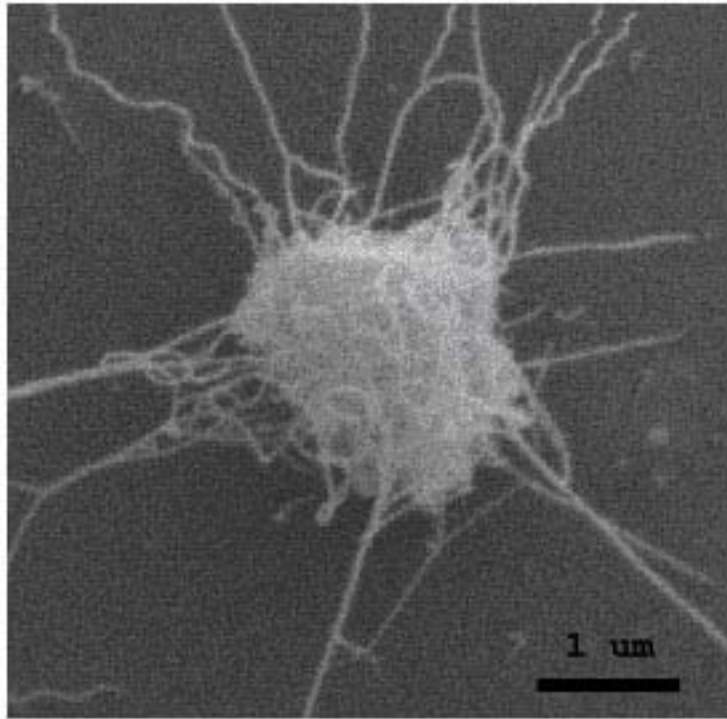


Figure 24 - Catalyst patch with nanotubes growing in all directions

Figure 24 shows a small patch of catalyst after CVD growth. It can be seen that tubes are sprouting from all sides of the catalyst. This creates a radius in which any other CNT devices would likely be rendered inoperative or shorted out. So, while CNT devices on their own may have a relatively small cost in substrate surface area, the extra tubes cause a larger effective area. This is illustrated in Figure 25.

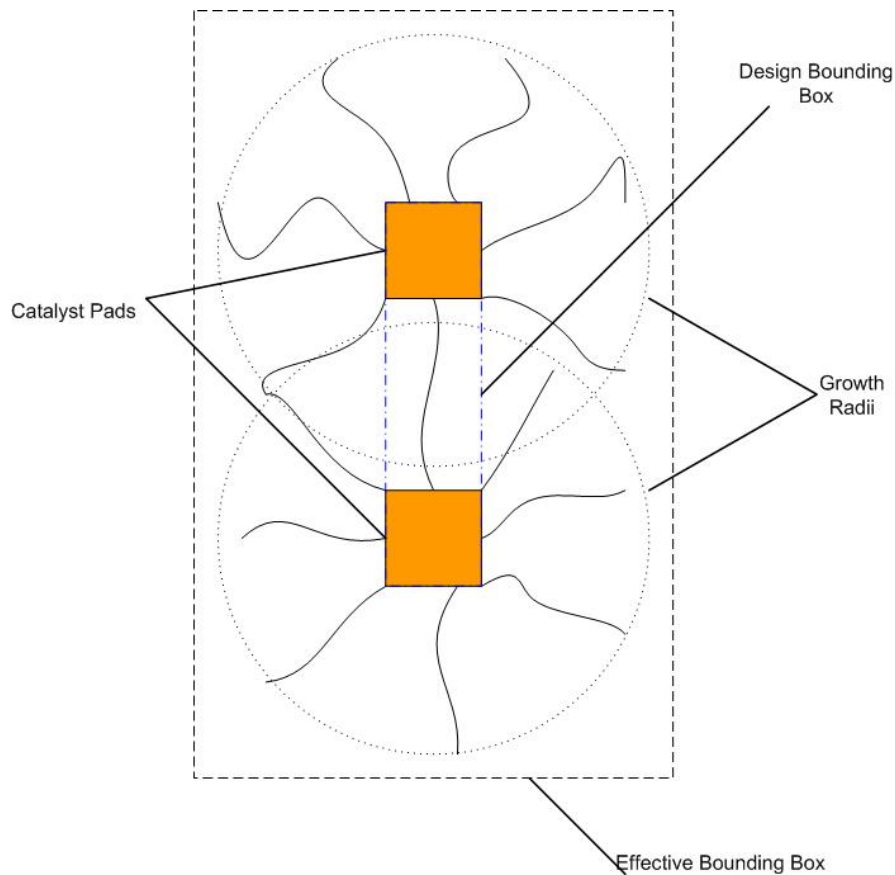


Figure 25 - While the surface area of a CNT device may be rather small, its effective surface area is much larger, due to the uncontrolled growth of unneeded tubes

This extra area will certainly outweigh any size benefit of CNT devices, and will likely outweigh any performance benefit. So a way must be found to contain or prevent these extra tubes.

A proposed means of containment is shown in Figure 26. A barrier region of alumina could be deposited in an arc around the catalyst patch. While alumina does not prevent CNT growth per se, it could possibly serve to at least contain the tubes somewhat. And while the effective surface area is larger than the device itself, it would be far less than without a barrier at all.

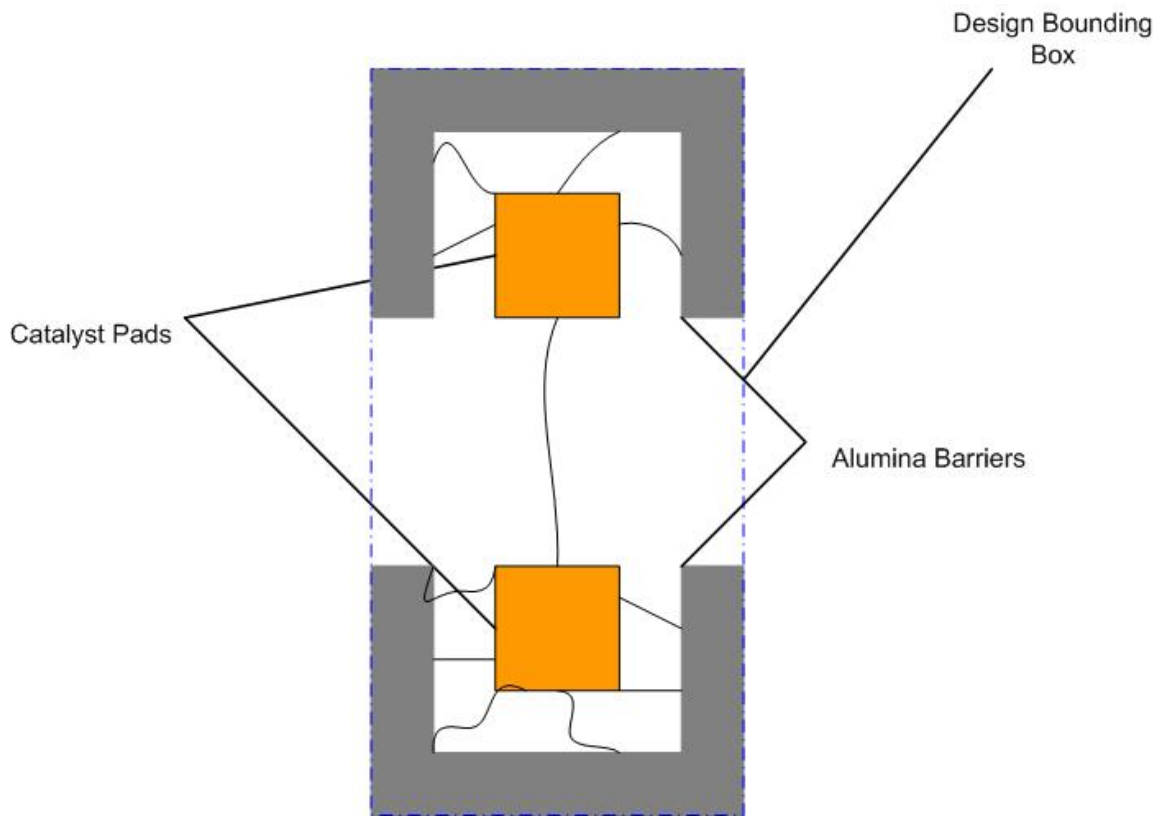


Figure 26 - A suggested means of containing extra CNTs

This idea could not be tested as part of this project. Another possibility would be to increase the flow rate. It is possible that a strong enough laminar flow could cause grown tubes to fall in the direction of the current.

3.10.6 Catalyst Thickness

Part of the difficulty in preparing samples for CVD is the application of the catalyst solution. For applying a uniform layer of liquid to a substrate, a spin-coater is typically used. However, the methanol-based solution used in this project evaporates very quickly. Often, the solution has evaporated before the spin coater has even reached full speed. This results in uneven layers of catalyst, which can cause changes in the frequency and size of nanotube bundles.

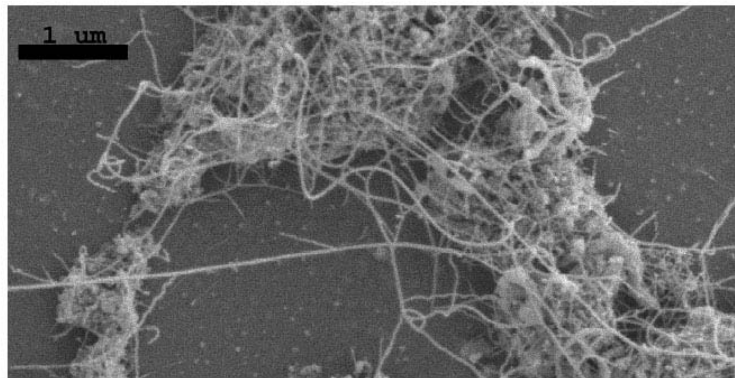
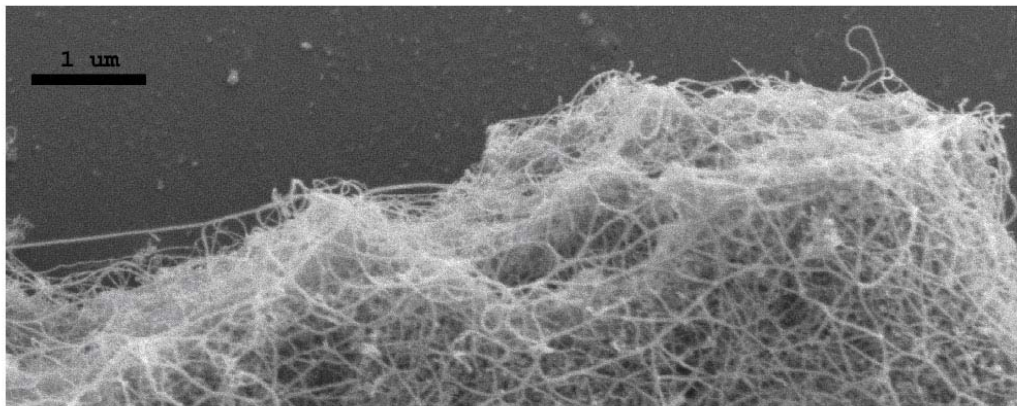


Figure 27 - The upper image shows a much thicker catalyst patch, and a resulting increase in the number of tubes. The lower image shows a thinner catalyst layer with fewer tubes.

As seen here, a thicker catalyst pad produces a larger number of tubes. This is only sensible, but underscores the fact that a way to achieve uniform catalyst thickness is essential for future applications.

Copyright © Stanton W McVay

4.0 Conclusions

4.1 Summary of Findings

A CVD reactor was built for this project, and single-walled carbon nanotubes were produced. These tubes were examined using both SEM and TEM microscopy. SEM was used to measure the length of relative frequency of grown nanotubes. TEM was used to confirm that the structures were indeed SWNTs, based on their crystal structure.

In terms of material cost, CVD is an inexpensive method for producing carbon nanotubes. The reactor built for this project cost less than \$2500.

One finding of this project is that previous research may have overstated the required methane flow rate for reliable nanotube growth. These results show that while a higher proportion of methane makes a small difference, a ratio of 20:380 sccm CH₄:Ar is sufficient to produce large numbers of tubes, of micron scale length.

Another factor unmentioned in previous works was the post-bake purging of the tube with argon. Without this step, amorphous carbon coats the nanotubes and everything else inside the reactor. While in hindsight it seems an obvious precaution, it was just this problem of coating that held up research for several weeks.

It was determined that 850 C is at or near an optimal temperature for growth of nanotubes, both in terms of number of tubes produced and length of tubes. For actual production, it may be desirable to use another temperature, if tight control of the number or length of tubes is needed. For example, 900 C was found to produce the least number of tubes per length of catalyst. To produce shorter tubes, growth at 800 C would be appropriate.

In general, longer reaction times do produce more tubes of greater length. However, it is also apparent across several trials that the majority of tubes are grown in less than 10 minutes. This would seem to indicate that the metal particles in the catalyst are of a narrow range of sizes and reached saturation at nearly the same time.

Earlier in the report, three problems facing widespread adoption of CNTs for electronics were stated: placement, numbers, and specificity. Based on this project, it appears that CVD is a good method for addressing the placement problem. Naturally, a few issues remain.

The largest obstacle is the tendency of the catalyst to sprout nanotubes in all directions. While CVD can certainly put a tube in a given location, it also tends to create lots of tubes in undesired places. This project did not test any means of preventing or containing these extra tubes. This would be a useful avenue for future research.

For the problem of numbers, these results are not especially consistent, which is a problem in itself. Some regions of a sample had large tangled masses of tubes while other regions had a few straight tubes. The formula and preparation of the catalyst solution could be improved, to provide more consistent results.

It should be noted that this work depended upon SEM and TEM imaging to confirm the presence and measure the characteristics of SWNTs. Other methods do exist to determine whether SWNTs are present. Some examples are Raman spectroscopy and x-ray diffraction. Also, atomic force microscopy (AFM) can be used to scan topography beyond the resolution limit of SEM. It may be useful to utilize these in future works, as TEM in particular was rather cumbersome to use.

4.2 Suggestions for Future Research

In no particular order, these are some difficulties found during the course of this project. It may be fruitful to future researchers to focus their effort in some of these areas.

- The catalyst solution in the project used a methanol base. This had a tendency to evaporate very quickly, which made spin-coating unreliable. Inconsistent spin-coating results in uneven catalyst thickness across a sample. A more stable solution would be very helpful, so long as it still evaporates in a reasonable amount of time.

- Mixing of the catalyst could also be improved. As noted, the grown tubes varied in density on the same sample. That is, one part of the catalyst might have just a handful of tubes while other parts had veritable webs of nanotubes. This would seem to indicate an inconsistency in the solution.

- Patterning of the catalyst was performed using optical lithography in this project. Most features thus produced were at least tens of microns to a side. For future work, electron beam lithography should be put to greater use.

- The nanotubes were found to grow from the catalyst in all directions. This is not a useful feature for microelectronics. A way must be found to either prevent or isolate these extra tubes, to minimize the surface area for a nanotube device, and to prevent shorts or other interference with nearby devices.

5.0 References

1. S. Iijima, "Helical nanotubules of graphitic carbon," *Nature*, vol 354, pp 56-58, 1991
2. R Saito, G. Dresselhaus, M. Dresselhaus, *Physical Properties of Carbon Nanotubes*. Imperial College Press, 2001.
3. A. Cassell, J. Raymakers, J. Kong, H. Dai, "Large Scale CVD Synthesis of Single-Walled Carbon Nanotubes," *J. Phys. Chem. B*, vol 103, pp6484-6492, 1999
4. R. Martel, T. Schmidt, H. Shea, T. Hertel, P. Avouris., "Single- and multi-wall carbon nanotube field-effect transistors," *App. Phys. Lett.*, vol 73, no 17, pp 2447-2449, 1998
5. P. Avouris, "Carbon Nanotube Electronics," *Chem. Phys.*, vol 281, pp 429-445, 2002
6. R. Martel, V. Derycke, C. Lavoie, J. Appenzeller, K. Chan, J. Tersoff, P. Avouris, "Ambipolar Electrical Transport in Semiconducting Single-Wall Carbon Nanotubes," *Phys. Rev. Lett.*, vol 87, no 25, pp 256805-(1-4), 2001
7. V. Derycke, R. Martel, J. Appenzeller, and P. Avouris, "Carbon nanotube Inter- and Intramolecular Logic Gates" *Nano Letters*, vol 1, no 9, pp 453-456, 2001
8. A. Javey, J. Guo, Q. Wang, M. Lundstrom, H. Dai, "Ballistic carbon nanotube field-effect transistors," *Nature*, vol 424, pp 654-655, 2003
9. J. Lee, C. Park, J. Kim, J. Kim, J. Park, K. Yoo, "Formation of low-resistance ohmic contacts between nanotube and metal electrodes by a rapid thermal annealing method," *J. Phys. D: Applied Physics*, vol 33, pp 1953-1956, 2000
10. A. Bachtold, M. Henny, C. Terrier, C. Strunk, C. Schoninger, J. Salvetat, J. Bonard, L. Forro, "Contacting carbon nanotubes selectively with low-ohmic contacts for four-probe electric measurements," *App. Phys. Lett.*, vol 73, pp 274-276, 1998
11. A. Bachtold, P. Hadley, T. Nakanishi, C. Dekker, "Logic Circuits with Carbon Nanotube Transistors," *Science*, vol 294, pp 1317-1320, 2001
12. W. Choi, S. Chee, E. Bae, J. Lee, B. Cheong, J. Kim, J. Kim, "Carbon-nanotube-based nonvolatile memory with oxide-nitride-oxide film and nanoscale channel," *App. Phys. Lett.*, vol 82, no 2, pp 275-277 (2003)
13. C. Journet, P. Bernier, "Production of carbon nanotubes," *App. Phys. A*, vol 67, pp 1-9, 1998
14. S. Farhat, M. Lamy de La Chapelle, A. Loiseau, C. Scott, S. Lefrant, C. Journet, P. Bernier, "Diameter control of single-walled carbon nanotubes using argon-helium mixture gases," *Jour. Chem. Phys.*, vol 115, no 14, pp 6752-6759, 2001
15. M. Keidar, A. Waas, "On the conditions of carbon nanotube growth in the arc discharge," *Nanotechnology*, vol 15, pp 1571-1575, 2004
16. P. Eklund, B. Pradhan, U. Kim, Q. Xiong, J. Fischer, A. Friedman, B. Holloway, K. Jordan, M. Smith, "Large-Scale Production of Single-Walled Carbon

- Nanotubes Using Ultrafast Pulses from a Free Electron Laser,” *Nano Letters*, vol 2, no 6, pp 561-566, 2002
17. W. Maser, E. Munoz, A. Benito, M. Martinez, G. de la Fuente, Y. Maniette, E. Anglaret, J. Sauvajol, “Production of high-density single-walled nanotube material by a simple laser-ablation method,” *Chem Phys Lett*, vol 292, pp 587-593, 1998
 18. Laser ablation schematic downloaded from <http://students.chem.tue.nl/ifp03/introduction.html>
 19. M. Yudasaka, R. Yamada, N. Sensui, T. Wilkins, T. Ichihashi, S. Iijima, “Mechanism of the Effect of NiCo, Ni and Co Catalysts on the Yield of Single-Wall Carbon Nanotubes Formed by Pulsed Nd:YAG Laser Ablation,” *J. Phys. Chem. B*, vol 103, pp 6224-6229, 1999
 20. R. Krupke, F. Hennrich, H. Lohneisen, M. Kappes, “Separation of Metallic from Semiconducting Single-Walled Carbon Nanotubes,” *Science*, vol 301, pp 344-347, 2003
 21. S. Rao, L. Huang, W. Setyawan, S. Hong, “Large-scale assembly of carbon nanotubes,” *Nature*, vol 425, pp 36-37, 2003
 22. J. Kong, H. Soh, A. Cassell, C. Quate, H. Dai, “Synthesis of individual single-walled carbon nanotubes on patterned silicon wafers,” *Nature*, vol 395, pp 878-881, 1998
 23. A. Harutyunyan, B. Pradhan, U. Kim, G. Chen, P. Eklund, “CVD Synthesis of Single Walled Carbon Nanotubes under “Soft” Conditions,” *Nano Letters*, vol 2, no 5, pp 525-530, 2002
 24. A. Cassell, J. Raymakers, J. Kong, H. Dai, “Large Scale CVD Synthesis of Single-Walled Carbon Nanotubes,” *J. Phys. Chem. B*, vol 103, no 31, pp 6482-6492, 1999
 25. C. Cheung, A. Kurtz, H. Park, C. Lieber, “Diameter-Controlled Synthesis of Carbon Nanotubes,” *J. Phys. Chem. B.*, vol 106, pp 2429-2433, 2002
 26. G. Tibbetts, “Growing Carbon Fibers with a Linearly Increasing Temperature Sweep: Experiments and Modelling,” *Carbon*, vol 30, no 3, pp 399-406, 1992

6.0 Vita – Stanton Wright McVay

Date and Place of Birth: May 2nd, 1976 in Charleston, WV

Colleges Attended: West Virginia University Institute of Technology
Montgomery, WV
Bachelor of Science in Electrical Engineering
Magna Cum Laude

University of Kentucky
Lexington, KY
Master of Science in Electrical Engineering

Professional Positions: Columbia Energy Group
Charleston, WV
Electrical Engineer

Rockwell-Collins, Inc.
Cedar Rapids, IA
Electrical Engineer